



euronoise

**Acoustics'08
Paris**
June 29-July 4, 2008

www.acoustics08-paris.org

Influence of solid phase elasticity in poroelastic liners submitted to grazing flows

Benoit Nennig, Jean-Daniel Chazot, Emmanuel Perrey-Debain and Mabrouk
Ben Tahar

Université de Technologie de Compiègne, Lab. Roberval UMR 6253, Dept. Acoustique, BP
60319, 60203 Compiègne, France
benoit.nennig@utc.fr

In this work, we study the sound propagation in a duct treated with a poroelastic liner exposed to a sheared grazing flow. Acoustic propagation in the fluid domain and in the liner is respectively governed by Galbrun's equation and Biot's model in the most general case.

In addition of using the complete Biot's model, simplified models are also tested. Bulk reaction approach that does not take into account solid phase elasticity and a model that neglects only the shear stress are hence used. These two simplified models enable to evaluate the contributions of the compressional and shear waves in the solid phase.

After some details on models and their numerical implementation, we shall illustrate these contributions on a silencer benchmark.

1 Introduction

Over the years, considerable effort has been directed toward the development of finite element models for predicting the propagation of sound waves in gas flow in the presence of acoustically treated walls. The practical applications of such work range from noise transmission in vehicle exhaust systems, through ventilation and air conditioning ducts, to the prediction of more complex three-dimensional fields in aeroacoustical configurations. In the early work dealing with the use of absorption finite elements, it was assumed that the liner was locally reacting, thus eliminating the need to discretize the absorbing material explicitly. Later, to illustrate the effects of a finite size bulk reacting lining, Craggs [6] derived a finite element model for porous materials where the solid phase was assumed to be infinitely rigid so that only compression waves are allowed to propagate and the material can be characterized by a complex wave number and a complex impedance. Until recently, most of the studies related to sound attenuation through dissipative silencers were carried out using this assumption and curiously enough, no attempt was made to quantify the effects of the finite stiffness of the absorbent material. Furthermore, the mean flow which is present in air moving ducts affects the upstream and downstream attenuation and this is usually taken into account by considering a uniformly moving flow in the central airway. This simplification of the flow field is made to ease the numerical treatment of the wave equation, but it has the drawback to neglect refraction in the boundary layer which is inevitably present in the vicinity of the walls. Because of these limitations, we think there is a need to develop more advanced numerical techniques based on the finite element methodology in order to incorporate these effects.

In this work, we present and compare three different finite element formulations to model the propagation in the poroelastic liner. These are based on (i) Biot's model where two longitudinal and one transverse wave types are present (ii) a simplified approach that neglects shear stress (iii) a bulk reacting material model. The acoustic propagation in the gas flow is written in terms of the Lagrangian displacement perturbation satisfying the Galbrun's equation [10]. As shown in this paper, this has the advantage of rendering the continuity conditions at the porous material/ airway interface more explicit and allows to define and easily compute the acoustic intensity across the interfaces of the fluid domain. To illustrate the method, we compute the Transmission Loss (TL) for typical dissipative silencers encountered in the automotive industry. In some cases, we show that the existence of multiple wave types in the porous material

can have significant consequences on the TL and that the liner is very sensitive to the boundary conditions that exist at its surface.

2 Formulation

2.1 Galbrun's equation

Galbrun's equation derives from general fluid mechanic conservation equations, whereby the linearization process is carried out with a lagrangian perturbation and involves only lagrangian displacement perturbation. However, the direct resolution of harmonic Galbrun's equation with the Finite Element Method (FEM) gives rise to corrupted results. To overcome this difficulty, the *mixed FEM formulation* has been introduced and extensively discussed in previous works [18, 9].

Under the assumption of homentropic perturbations and eulerian flow, the equation can be written in the frequency domain ($e^{-i\omega t}$) as follows :

$$\begin{cases} -\rho_0\omega^2\mathbf{w} - 2i\omega\rho_0\mathbf{v}_0 \cdot \nabla\mathbf{w} \\ + \rho_0\mathbf{v}_0 \cdot \nabla(\mathbf{v}_0 \cdot \nabla\mathbf{w}) + \nabla p^L = 0, \\ p^L + \rho_0c_0^2\nabla \cdot \mathbf{w} = 0. \end{cases} \quad (1)$$

Here, subscripts "0" denotes the mean flow variables, p^L is the lagrangian acoustic pressure and \mathbf{w} the lagrangian displacement perturbation. The associated weak formulation is

$$\begin{aligned} & -\int_{\Omega_a} \frac{1}{\rho_0c_0^2} p^{L*} p^L \, d\Omega + \int_{\Omega_a} \nabla p^{L*} \cdot \mathbf{w} \, d\Omega + \int_{\Omega_a} \mathbf{w}^* \cdot \nabla p^L \, d\Omega \\ & -\omega^2 \int_{\Omega_a} \rho_0 \mathbf{w}^* \cdot \mathbf{w} \, d\Omega - \int_{\Omega_a} \rho_0 (\mathbf{v}_0 \cdot \nabla \mathbf{w}^*) \cdot (\mathbf{v}_0 \cdot \nabla \mathbf{w}) \, d\Omega \\ & -i\omega \int_{\Omega_a} \rho_0 \mathbf{w}^* \cdot (\mathbf{v}_0 \cdot \nabla \mathbf{w}) \, d\Omega + i\omega \int_{\Omega_a} \rho_0 (\mathbf{v}_0 \cdot \nabla \mathbf{w}^*) \cdot \mathbf{w} \, d\Omega \\ & + \underbrace{\int_{\partial\Omega_a} \mathbf{w}^* \cdot \left\{ \rho_0 (\mathbf{v}_0 \cdot \mathbf{n}_a) \frac{d\mathbf{w}}{dt} \right\}}_{I_1} dS - \int_{\partial\Omega_a} p^{L*} (\mathbf{w} \cdot \mathbf{n}_a) \, dS \\ & = 0, \quad \forall \{ \mathbf{w}^*, p^{L*} \}, \end{aligned} \quad (2)$$

where p^{L*} , \mathbf{w}^* are the test functions and \mathbf{n}_a denotes the outward normal unit vector. The discretisation in the three dimensional case has been carried out by Bériot *et al.* [3]. Interpolation is linear for the pressure and a bubble function is added for the displacement in order to respect the inf-sup condition.

2.2 Biot's equations

For isotropic porous materials, Biot's model [4] is grounded on the superposition of a fluid phase and a solid

phase which are coupled together. The original equations set involves the fluid phase displacement \mathbf{U} and the solid phase displacement \mathbf{u} . For the numerical implementation, the equivalent Atalla's mixed formulation [2] will be used to simplify coupling conditions and to save computation time. Indeed, for linear element, only 4 degrees of freedom (dof) per node are needed instead of 6 in the (\mathbf{u}, \mathbf{U}) formulation. The Atalla's mixed formulation as presented in [2] is

$$\begin{cases} \nabla \cdot \underline{\underline{\sigma}}^s(\mathbf{u}) + \omega^2 \rho \mathbf{u} + \gamma \nabla p = 0, \\ \Delta p + \omega^2 \frac{\rho_{22}}{R} p - \omega^2 \frac{\rho_{22}}{\phi^2} \gamma \nabla \cdot \mathbf{u} = 0. \end{cases} \quad (3)$$

Here, p is the pressure in the fluid phase and \mathbf{u} is the solid phase displacement vector, $\gamma = \phi \left(\frac{\rho_{12}}{\rho_{22}} - \frac{Q}{R} \right)$ and

$$\rho = \rho_{11} - \frac{\rho_{12}^2}{\rho_{22}}.$$

The associated weak formulation, considering the test function p^* and \mathbf{u}^* , is

$$\begin{aligned} & \int_{\Omega_p} \underline{\underline{\sigma}}^s(\mathbf{u}) : \underline{\underline{\epsilon}}(\mathbf{u}^*) \, d\Omega - \rho \omega^2 \int_{\Omega_p} \mathbf{u} \cdot \mathbf{u}^* \, d\Omega \\ & + \int_{\Omega_p} \left[\frac{\phi^2}{\omega^2 \rho_{22}} \nabla p \cdot \nabla p^* - \frac{\phi^2}{R} p p^* \right] \, d\Omega \\ & - \int_{\Omega_p} \left[\gamma + \phi \left(1 + \frac{Q}{R} \right) \right] (\nabla p^* \cdot \mathbf{u} + \nabla p \cdot \mathbf{u}^*) \, d\Omega \\ & - \phi \left(1 + \frac{Q}{R} \right) \int_{\Omega_p} (p^* \nabla \cdot \mathbf{u} + p \nabla \cdot \mathbf{u}^*) \, d\Omega \\ & - \int_{\partial\Omega_p} \left[\underline{\underline{\sigma}}^t \cdot \mathbf{n} \right] \cdot \mathbf{u}^* \, dS - \int_{\partial\Omega_p} \phi (U_n - u_n) p^* \, dS \\ & = 0, \quad \forall \{p^*, \mathbf{u}^*\}, \end{aligned} \quad (4)$$

where, \mathbf{n} denotes the outward normal unit vector to the poroelastic domain and ϕ the porosity. A, N, P, Q, R are Biot's coefficients as defined in [4, 1]. A and N correspond to the Lamé coefficients and $P = A + 2N$. R is the bulk modulus of the fluid phase and Q indicates the coupling of the two phases volumic dilatation. We can note that the imaginary part of A and N includes the structural damping and, in Q and R this part includes the thermal dissipation. Those parameters are related to the material properties given in Table 1 by the Allard formulation [1].

2.3 Formulation without shear stress

Different simplifications can be brought to the previous full Biot's theory depending on the studied material elastic characteristics. A simplification was hence proposed by Chazot *et al.* in [5] to model light and non cohesive poroelastic materials. The basic idea of this model is to modify the elastic law of the solid phase to suppress shear stresses. The solid phase is then assumed to behave like a fluid. The resulting fluid-fluid model (FF) is

$$\begin{cases} [A \Delta p_s + p_s] + B \Delta p = 0 \\ [C \Delta p + p] + D \Delta p_s = 0. \end{cases} \quad (5)$$

Here, p_s is the equivalent pressure in the solid phase while elastic coefficients A, B, C and D are

$$\begin{aligned} A &= F(P\rho_{22} - Q\rho_{12}), & B &= F(-P\rho_{12} + Q\rho_{11})\phi/(1-\phi), \\ C &= F(-Q\rho_{12} + R\rho_{11}), & D &= F(Q\rho_{22} - R\rho_{12})(1-\phi)/\phi, \\ F &= [(\rho_{22}\rho_{11} - \rho_{12}^2)\omega^2]^{-1}. \end{aligned} \quad (6)$$

They are related to elastic and inertial coupling coefficients. Q, R, ϕ , and ρ_{ij} are unchanged compared to those used in Biot's formulation. However, two different definitions can be employed for the elastic coefficient P . If one considers a light and non cohesive granular material without shear stress, the elastic coefficient P stands for the skeleton bulk modulus with a coupling part due to the fluid phase : $P = K_b + \frac{(1-\phi)^2}{\phi} K_f$. On the contrary, when the aim is to neglect the shear stress in a material with a large shear modulus N , it is also possible to keep the same coefficient P than the one used in Biot's formulation: $P = \frac{4}{3}N + K_b + \frac{(1-\phi)^2}{\phi} K_f$. This enables to keep the same dispersion equation in both formulations. Physically, in the first case, the energy is totally distributed in the solid and fluid longitudinal waves, while in the second case the energy part of the solid shear wave is not re-distributed but simply neglected. Of course, when N is very small, both definitions of P become identical. The second definition of P is used here. The associated weak formulation for the fluid fluid model is given here:

$$\begin{aligned} & \int_{\Omega_p} (-A \nabla p_s \cdot \nabla p_s^* + p_s p_s^*) \, d\Omega + \int_{\partial\Omega_p} A p_s^* \nabla p_s \cdot \mathbf{n} \, dS \\ & - \int_{\Omega_p} (B \nabla p \cdot \nabla p_s^*) \, d\Omega + \int_{\partial\Omega_p} B p_s^* \nabla p \cdot \mathbf{n} \, dS \\ & + \int_{\Omega_p} (-C \nabla p \cdot \nabla p^* + p p^*) \, d\Omega + \int_{\partial\Omega_p} C p^* \nabla p \cdot \mathbf{n} \, dS \\ & - \int_{\Omega_p} (D \nabla p_s \cdot \nabla p_s^*) \, d\Omega + \int_{\partial\Omega_p} D p_s^* \nabla p_s \cdot \mathbf{n} \, dS \\ & = 0, \quad \forall \{p_s^*, p^*\}, \end{aligned} \quad (7)$$

where \mathbf{n} denotes here the outward normal unit vector to the poroelastic domain. The discretisation is done with linear elements.

2.4 Bulk reacting modeling

An other classical simplification of Biot's model is to consider the skeleton as totally rigid [1, 13, 8, 17, 15]. The solid phase elasticity is then neglected, and only the fluid phase is modeled. Viscous and thermal effect are however still taken into account via an equivalent fluid density $\rho_e = \rho_{22}/\phi$, and an equivalent acoustic celerity $c_e = (K_f/\rho_e)^{1/2}$. Here, the same frequency dependent expressions of K_f and ρ_{22} used in Biot's model and based on Allard's formulation are employed in the bulk material modeling (BM). Finally, the weak formulation is standard and linear elements are used.

3 Matching of the acoustic-elastic field

3.1 Continuity Conditions

Continuity conditions without flow are summarized by Debergue *et al.* [7] for several configurations. Here, we shall focus on a "direct" coupling, without impermeable membrane or perforate sheet, but there is no hindrance to implement them. Indeed, perforated sheet can be included thanks to its impedance as a pressure jump and

its implementation is straight forward because of the mixed formulation.

The first condition, given by (8), stems from the standard continuity requirement of the normal stress at the interface. Conditions (9,10), ensures the continuity of the pressure and the continuity of the mass flux at the interface.

$$[\underline{\sigma}^t \mathbf{n}] = -p^L \cdot \mathbf{n}, \quad (8)$$

$$p = p^L, \quad (9)$$

$$\mathbf{w} \cdot \mathbf{n} = w_n = \phi(U_n - u_n) + u_n. \quad (10)$$

In the presence the flow, the classical cinematic condition is the continuity of the displacement and all the dynamical conditions remain valid so the same set of coupling condition can be use unambiguously.

3.2 Numerical implementation

3.2.1 Galbrun - Biot

Firstly, the I_1 integral in (2) vanishes on Γ because there is no flow in the liner, vectors \mathbf{v}_0 and \mathbf{n}_a are orthogonal. Both conditions (8) and (10) are directly substituted in boundary terms. But, as for Biot-Helmholtz coupling, the second condition (9) can not be imposed in the weak formulation. Some authors have resorted to Lagrange multipliers or imposed directly the relation in the system. Here, we introduce an additional functional

$$\int_{\Gamma} w_n^* (p^L - p) \, d\Gamma = 0, \quad \forall \{w_n^*\}, \quad (11)$$

and w_n^* plays the same role as a Lagrange multiplier but avoids the additional dof. As this condition is added directly in the formulation we could relax the constraint in (9) and replace p^L by p . Those two manipulations give on Γ

$$\int_{\Gamma} p \cdot u_n^* \, d\Gamma + \int_{\Gamma} p^* \cdot u_n \, d\Gamma + \int_{\Gamma} p^L \cdot w_n^* \, d\Gamma + \int_{\Gamma} p^{L*} \cdot w_n \, d\Gamma - \int_{\Gamma} p^* \cdot w_n \, d\Gamma - \int_{\Gamma} w_n^* \cdot p \, d\Gamma = 0, \quad \forall \{p^*, u_n^*, p^{L*}, w_n^*\}. \quad (12)$$

The first line of (12) shows the pressure - displacement coupling in each domain whereas the second gives pressure - displacement coupling between the two domains. It's worth observing that this coupling produces a symmetric operator between lagrangian displacement \mathbf{w} and the fluid pressure in the porous.

3.2.2 Galbrun - FF model

Coupling conditions between acoustic and porous domains are similar to coupling condition used in Biot's formulation, but taking into account the simplified FF form of $\underline{\sigma}^t$ in (8), we have

$$p^L = (1 - \phi)p_s + \phi p. \quad (13)$$

Solid and fluid porous displacements in the last coupling condition can then be related to solid and fluid pressure gradients

$$\mathbf{u} = I \nabla p_s + J \nabla p, \quad (14)$$

$$\mathbf{U} = K \nabla p_s + L \nabla p, \quad (15)$$

with the intermediate coefficients I, J, K and L given by

$$\begin{aligned} I &= F(1 - \phi) \rho_{22}, & J &= -F \phi \rho_{12}, \\ K &= -F(1 - \phi) \rho_{12}, & L &= F \phi \rho_{11}. \end{aligned} \quad (16)$$

However, in order to avoid the calculation of pressure gradients at boundary surfaces, Lagrange multipliers are used instead of solid and fluid normal pressure gradients

$$\lambda_s = \nabla p_s \cdot \mathbf{n}, \quad \text{and} \quad \lambda_f = \nabla p \cdot \mathbf{n}. \quad (17)$$

The condition (10) can then be imposed directly in (2) boundary term by replacing w_n by $(1 - \phi)(I\lambda_s + J\lambda_f) + \phi(K\lambda_s + L\lambda_f)$. However, to impose the two conditions (13,9), two additional functionals are introduced, using Lagrange multipliers

$$\int_{\Gamma} \lambda_s^* (p^L - p_s) \, dS, \quad \int_{\Gamma} \lambda_f^* (p^L - p_f) \, dS. \quad (18)$$

Finally, boundary terms with pressure gradients in (7) are also written with Lagrange multipliers

$$\int_{\Gamma} (Ap_s^* + Dp^*)\lambda_1 + (Bp_s^* + Cp^*)\lambda_2 \, dS. \quad (19)$$

3.2.3 Galbrun - Bulk reacting modeling

In the case of bulk reacting modeling, it remains only the two coupling condition

$$p = p^L \quad (20)$$

$$w_n = U_n \quad (21)$$

The second coupling condition (21) is imposed directly in the porous boundary term by replacing U_n by w_n , while the first one (20) is imposed with the additional functional given in (11) as in the Galbrun-Biot case. Finally, boundary and coupling terms writes

$$\int_{\Gamma} p^{L*} w_n \, dS + \int_{\Gamma} w_n^* p^L \, dS - \int_{\Gamma} w_n p^* \, dS - \int_{\Gamma} w_n^* p \, dS = 0. \quad (22)$$

4 Power balance

4.1 Intensity with shear flow

To characterize acoustical materials, the access to power balance can be a useful design and comprehension tool. Whereas linearized Euler's equations are conservative only for irrotational flow and isentropic flow [12] Galbrun's equation can be written as an exact conservation law for homentropic sheared flow. It's worth noting that the conservation law is not unique and we shall use here the expression of intensity (23) given by Godin [11] and Peyret *et al.* [16]

$$\mathcal{I} = \rho_0 \left(\frac{\partial \mathbf{w}}{\partial t} \cdot \frac{d\mathbf{w}}{dt} \right) \mathbf{v}_0 + (p^L - \mathbf{w} \cdot \nabla p_0) \frac{\partial \mathbf{w}}{\partial t}. \quad (23)$$

This equation describes the energy flux (*i.e.* intensity) due to acoustical and hydrodynamical perturbation which are coupled in the case of a shear flow.

This expression can be easily computed after the resolution. We should mention that with linear element used

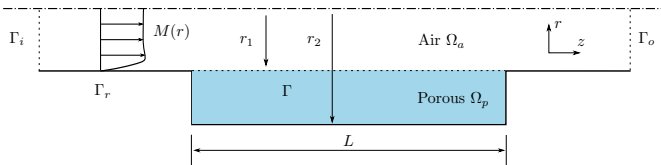
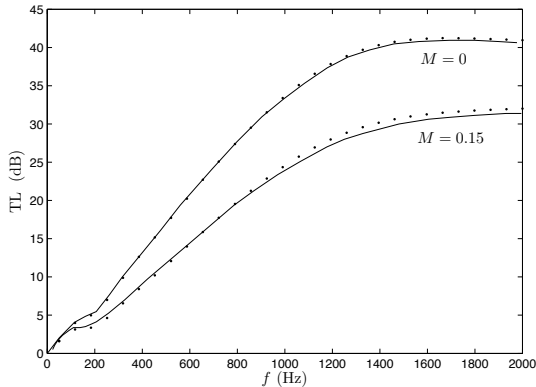


Figure 1: Geometry of the silencer benchmark

Figure 2: Kirby validation case for $M = 0$ and $M = 0.15$, \cdots FEM, — Kirby [14].

here intensity will be constant on each element, because intensity involves gradient in the material derivative. The power is deduced from flux of intensity across the acoustic domain non-rigid boundary, the flux across Γ_o , Γ , Γ_i gives respectively the transmitted power \mathcal{P}_t , the absorbed \mathcal{P}_{abs} and the reflected power \mathcal{P}_r , because \mathcal{P}_i is known. The TL is defined by

$$TL = 10 \log \left(\frac{\mathcal{P}_t}{\mathcal{P}_i} \right). \quad (24)$$

4.2 Boundary conditions at duct ends

As the diameter of the inlet and the outlet is quite small, far away from the discontinuity only the first mode is propagative, this remark allows simple boundary condition. At the outlet Γ_o , the non reflective condition is assured by the modal impedance of the first mode (expressed in term of the acoustic displacement) given by the resolution of Pridmore-Brown equation as proposed by Treysède [18]. At the inlet Γ_i , the degrees of freedom are expressed in terms of the incident and the reflected mode amplitude and the linear system is rearranged to set the amplitude of the incident wave.

4.3 Validation

A validation has been carried out for the configuration, depicted on Fig. 1, proposed by Kirby [14] ($r_1 = 37$ mm, $r_2 = 76.6$ mm, $L = 315$ mm) with a fibrous material (“E-glass”) with the bulk reacting model and a very good agreement can be seen on the Fig. 2. This model will constitute our reference in the high frequency domain.

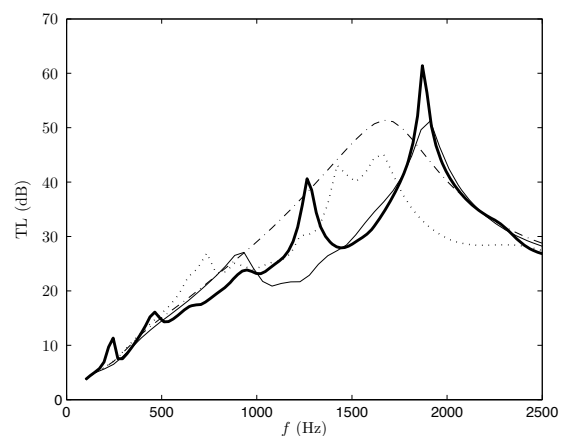
4.4 Numerical benchmark

A numerical study has been carried out for the Kirby’s configuration for different kind of porous material listed

Properties	Units	XFM
ϕ	[-]	0.98
σ	[kNm ⁻⁴ s]	13.5
α_{inf}	[-]	1.7
Λ	[μ m]	80
Λ'	[μ m]	160
ρ_1	[kgm ⁻³]	30
E	[kPa]	540(1 - 0.05i)
ν	[-]	0.35

Table 1: Materials properties used in numerical tests

in Table 1. For the XFM foam, the transmission loss given Fig. 3 illustrates the influence of the skeleton. Indeed the three models yield significant differences on the results. Firstly, Biot’s model presents many resonance peaks in both tested configurations (*clamped* and *sliding*). In the *sliding* case, a good agreement can be seen above 1500 Hz with the FF model in particular with an excellent description of the 2000 Hz phenomenon probably due to a compressional wave effect. However, the 1300 Hz peak is absent with the FF model, that’s why we are tempted to attribute it to shear effects but complementary tests are under investigation. The differences between *sliding* and *clamped* cases are significant and highlight the installation effects. It’s worth noting that the FF model can not describe the clamped boundary condition just as the bulk reacting modeling because the shear stress is neglected. Finally, for this configuration and this foam, the bulk reacting modeling is a too simplified approach. In the presence of a sheared flow Fig. 4, similar conclusions can be drawn, but resonance peaks are less pronounced and shifted to the lower frequency due to convection effect.

Figure 3: Confrontation between the three models on the XFM foam without flow : — Biot sliding, --- FF, - - - BM, \cdots Biot clamped.

5 Conclusion and prospects

These first results are engaging as they clearly show differences between poroelastic models. They also allow us to observe effects due to the presence of the mean flow, boundary conditions of the porous material and

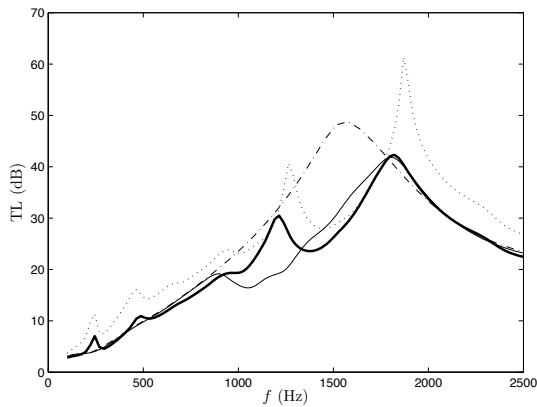


Figure 4: Confrontation between the three models on the XFM foam with sheared flow $\overline{M}(r) = 0.18$:
 — Biot sliding, — FF, - - - BM, · · · Biot sliding without flow.

the skeleton resonance. Neglecting shear may be in some cases an interesting approach for saving computation time and may offer a better description of phenomenon than the standard bulk reaction model in some specific muffler applications.

The finite element model presented in this work provides an accurate numerical tool to identify compression and shear wave effects. More work is going-on, in particular, a more physics-based approach is being carried out in order to find a good criterion to establish the FF model application range.

References

- [1] J.-F. Allard. *Propagation of Sound in Porous Media: Modeling Sound Absorbing Materials*. Chapman and Hall, 1993.
- [2] N. Atalla, M. A. Hamdi, and R. Panneton. Enhanced weak integral formulation for the mixed (u, p) poroelastic equations. *J. Acoust. Soc. Am.*, 109(6):3065 – 3068, 2001.
- [3] H. Bériot and M. Ben Tahar. A three dimensional finite element model for sound propagation in non potential mean flows. In *Proceedings of ICSV13*, Vienna, Austria, July 2-6, 2006.
- [4] M.A. Biot. Theory of propagation of elastic waves in a fluid-saturated porous solid. i. low-frequency range. *J. Acoust. Soc. Am.*, 28(2):168–178, 1956.
- [5] J. D. C. Chazot and J. L. G. Guyader. Characterization of light and non cohesive poro-granular materials with a fluid/fluid model. *Acta Mech.*, 195(1-4):227–247, 2008.
- [6] A. Craggs. A finite element model for rigid porous absorbing materials. *J. Sound Vib.*, 61(1):101–101, 1978.
- [7] P. Debergue, R. Panneton, and N. Atalla. Boundary conditions for the weak formulation of the mixed (u, p) poroelasticity problem. *J. Acoust. Soc. Am.*, 106(5):2393–2390, 1999.
- [8] M.E. Delany and E.N. Bazley. Acoustical properties of fibrous asorbent materials. *Appl. Acoust.*, 3(2), April 1970.
- [9] G. Gabard, F. Treyssède, and M. Ben Tahar. A numerical method for vibro-acoustic problems with sheared mean flows. *J. Sound Vib.*, 272:991–1011, 2004.
- [10] H. Galbrun. *Propagation d'une onde sonore dans l'atmosphère terrestre et théorie des zones de silence*. Gauthier-Villars, 1931.
- [11] O.A. Godin. Reciprocity and energy theorems for waves in a compressible inhomogeneous moving fluid. *Wave motion*, 25(2):143–167, 1997.
- [12] M. E. Goldstein. *Aeroacoustics*. 1976.
- [13] D.L. Johnson, T.J. Plona, and C. Scala. Tortuosity and acoustic slow waves. *Phys. Rev. Lett.*, 49(25):1840–1844, 1982.
- [14] R. Kirby. Simplified techniques for predicting the transmission loss of a circular dissipative silencer. *J. Sound Vib.*, 243(3):403–426, 2001.
- [15] D. Lafarge, P. Lemarinier, and J.F. Allard. Dynamic compressibility of air in porous structures at audible frequencies. *J. Acoust. Soc. Am.*, 102(4):1995–2006, 1997.
- [16] C. Peyret and G. Elias. Finite-element method to study harmonic aeroacoustics problems. *J. Acoust. Soc. Am.*, 110(2):661–668, 2001.
- [17] M.R. Stinson and Y. Champoux. Propagation of sound and the assignment of shape factors in model porous materials having simple pore geometries. *J. Acoust. Soc. Am.*, 91(2):685–695, 1992.
- [18] F. Treyssède, G. Gabard, and M. Ben Tahar. A mixed finite element method for acoustic wave propagation in moving fluids based on an eulerian lagrangian description. *J. Acoust. Soc. Am.*, 113(2):705–716, 2003.